Chiral perturbation approach to the $pp \to pp\pi^0$ reaction near threshold

B.-Y. Park,* F. Myhrer, J. R. Morones, T. Meissner, and K. Kubodera
Department of Physics and Astronomy, University of South Carolina, Columbia, South Carolina 29208
(Received 18 December 1995)

The usual theoretical treatments of the near-threshold $pp \to pp\pi^0$ reaction are based on various phenomenological Lagrangians. In this work we examine the relationship between these approaches and a systematic chiral perturbation method. Our chiral perturbation calculation indicates that the pion rescattering term should be significantly enhanced as compared with the traditional phenomenological treatment, and that this term should have substantial energy and momentum dependence. An important consequence of this energy-momentum dependence is that, for a representative threshold kinematics and within the framework of our semiquantitative calculation, the rescattering term interferes destructively with the Born term in sharp contrast to the constructive interference obtained in the conventional treatment. This destructive interference makes theoretical cross sections for $pp \to pp\pi^0$ much smaller than the experimental values, a feature that suggests the importance of the heavy-meson exchange contributions to explain the experimental data.

PACS number(s): 13.75.Cs, 13.75.Gx, 12.39.Fe

I. INTRODUCTION

Recently Meyer *et al.* [1] carried out high-precision measurements of the total cross sections near threshold for the reaction

$$p + p \to p + p + \pi^0. \tag{1}$$

These measurements were confirmed by Bondar *et al.* [2]. The early theoretical calculations [3–5] underestimate these s-wave π^0 production cross sections by a factor of ~ 5.

The basic features of these early calculations may be summarized as follows. The pion production reactions are assumed to be described by the single nucleon process (the Born term), Fig. 1(a), and the s-wave pion rescattering process, Fig. 1(b). The π-N vertex for the Born term is assumed to be given by the pseudovector interaction Hamiltonian

$$\mathscr{H}_0 = \frac{g_A}{2f_\pi}\bar{\psi}\left(\boldsymbol{\sigma}\cdot\nabla(\boldsymbol{\tau}\cdot\boldsymbol{\pi}) - \frac{i}{2m_N}\{\boldsymbol{\sigma}\cdot\nabla, \boldsymbol{\tau}\cdot\dot{\boldsymbol{\pi}}\}\right)\psi, \tag{2}$$

where g_A is the axial coupling constant, and $f_\pi = 93$ MeV is the pion decay constant. The first term represents p-wave pion-nucleon coupling, while the second term accounts for the nucleon recoil effect and makes $\mathscr{H}_0$ "Galilean invariant." For s-wave pion production only the second term contributes. Since this second term is smaller than the first term by a factor of $\sim m_\pi/m_N$, the contribution of the Born term to s-wave pion production is intrinsically suppressed, and as a consequence the process becomes sensitive to two-body contributions, Fig. 1(b). The s-wave rescattering vertex in Fig. 1(b) is commonly calculated using the phenomenological Hamiltonian [3]

$$\mathscr{H}_1 = 4\pi\frac{\lambda_1}{m_\pi}\bar{\psi}\boldsymbol{\pi}\cdot\boldsymbol{\pi}\psi + 4\pi\frac{\lambda_2}{m_\pi^2}\bar{\psi}\boldsymbol{\tau}\cdot\boldsymbol{\pi}\times\dot{\boldsymbol{\pi}}\psi. \tag{3}$$

The two coupling constants λ_1 and λ_2 in Eq. (3) were determined from the S_{11} and S_{31} pion nucleon scattering lengths $a_{1/2}$ and $a_{3/2}$ as

$$\lambda_1 = \frac{m_\pi}{6}\left(1 + \frac{m_\pi}{m_N}\right)(a_{1/2} + 2a_{3/2}), \tag{4a}$$

$$\lambda_2 = \frac{m_\pi}{6}\left(1 + \frac{m_\pi}{m_N}\right)(a_{1/2} - a_{3/2}). \tag{4b}$$

The current algebra prediction [6] for the scattering lengths, $a_{1/2} = -2a_{3/2} = m_\pi/4\pi f_\pi^2 = 0.175 m_\pi^{-1}$, implies that only chiral symmetry breaking terms will give a nonvanishing value of the coupling constant λ_1 in Eq. (3). Therefore λ_1 is expected to be very small. Indeed, the empirical values $a_{1/2} \simeq 0.175 m_\pi^{-1}$ and $a_{3/2} \simeq -0.100 m_\pi^{-1}$ obtained by Höhler *et al.* [7] lead to $\lambda_1 \sim 0.005$ and $\lambda_2 \sim 0.05$. So the contribution of the λ_1 term in Eq. (3) is significantly suppressed. Meanwhile, although λ_2 is much larger than λ_1, the isospin structure of the λ_2 term is such that it cannot contribute to the π^0 production from two protons at the rescattering vertex in Fig. 1(b). Thus the use of the phenomenological Hamiltonians, Eqs. (2) and (3), to calculate the Born term and the rescattering terms illustrated in Figs. 1(a) and 1(b), gives significantly suppressed cross sections for the $pp \to pp\pi^0$ reaction near threshold. Therefore, theoretically calculated cross sections can be highly sensitive to any deviations from this conventional treatment. These delicate features should be kept in mind in discussing the large discrepancy (a factor of ~ 5) between the observed cross sections and the predictions of the earlier calculations.

A plausible mechanism to increase the theoretical cross section was suggested by Lee and Riska [8]. They proposed to supplement the contribution of the pion-exchange diagram, Fig. 1(b), with the contributions of the short-range axial-charge exchange operators which were directly related to heavy-meson exchanges in the nucleon-nucleon interactions [9]. According to Lee and Riska, the shorter-range meson exchanges (scalar and vector exchange contributions)

*On leave of absence from Department of Physics, Chungnam National University, Daejeon 305-764, Korea.

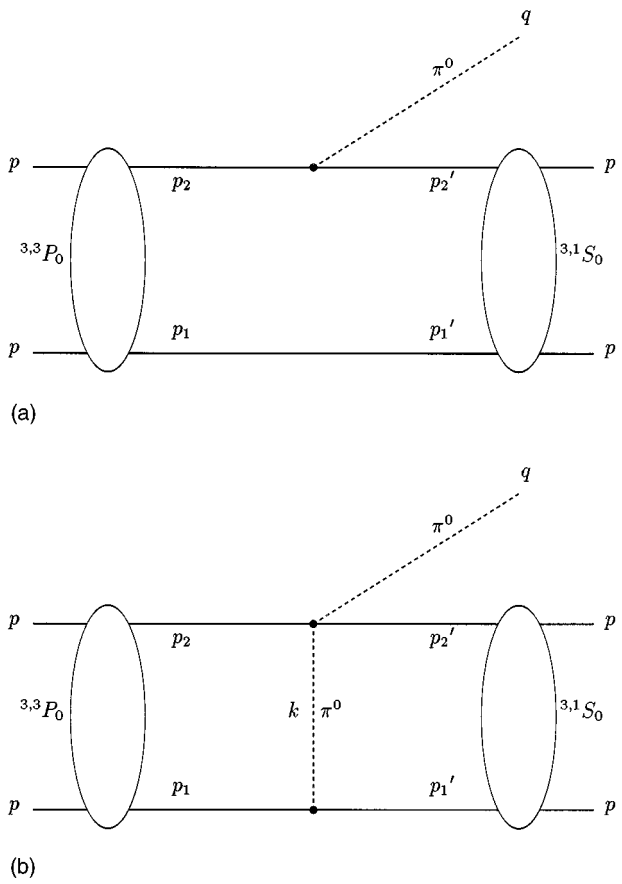

FIG. 1. Single nucleon process (Born term) (a) and pion rescattering process (b) for the $pp \to pp\pi^0$ reaction near threshold. ${}^{2T+1,2S+1}L_J$ denotes the isospin and angular momenta of the initial and final states.

can enhance the cross section by a factor 3–5. Subsequently, Horowitz *et al.* [10] demonstrated, for the Bonn meson exchange potential, a prominent role of the σ meson in enhancing the cross section, thereby basically confirming the conclusions of Lee and Riska. The possible importance of heavy-meson exchanges may be inferred from the following simple argument. Consider Fig. 1(b) in the center-of-mass (CM) system with the initial and final interactions turned off and with the exchanged particle allowed to be any particle (not necessarily a pion). At threshold, $q_0 = m_\pi$, $\boldsymbol{q} = 0$, $\boldsymbol{p}_1' = \boldsymbol{p}_2' = 0$, so that any exchanged particle must have $k_0 = m_\pi/2 = 70$ MeV and $|\boldsymbol{k}| = \sqrt{m_\pi m_N + (m_\pi/2)^2} \sim 370$ MeV/c, which implies $k^2 = -m_\pi m_N$. Thus the rescattering process probes two-nucleon forces at distances $\sim$ 0.5 fm corresponding to a typical effective exchanged mass $\sqrt{m_\pi m_N} = 370$ MeV. Its sensitivity to the intermediate-range *N-N* forces indicates the possible importance of the two-body heavy meson axial exchange currents considered by Lee and Riska. The particular kinematical situation we considered here shall be referred to as the *typical threshold kinematics*.

Meanwhile, Hernández and Oset [11] considered the *off-shell* dependence of the πN *s*-wave isoscalar amplitude featuring in the rescattering process, Fig. 1(b). They pointed out that the *s*-wave amplitude could be appreciably enhanced for off-shell kinematics pertinent to the rescattering process. We have seen above that, for the *typical threshold kinematics*, the exchanged pion can indeed be far off shell. The actual kinematics of course may deviate from the *typical threshold kinematics* rather significantly due to energy-momentum exchanges between the two nucleons in the initial and final states, but the importance of the off shell kinematics for the exchanged pion is likely to persist. Hernández and Oset examined two types of off-shell extrapolation: (i) the Hamilton model for πN isoscalar amplitude based on σ exchange plus a short range piece [12], and (ii) an extrapolation based on the current algebra constraints. In either case the enhancement of the total cross section due to the rescattering process was estimated to be strong enough to reproduce the experimental data. A more detailed momentum-space calculation carried out by Hanhart *et al.* [13] supports the significant enhancement due to an off-shell effect in the rescattering process, although the enhancement is not large enough to explain the experimental data. It should be emphasized that Hanhart *et al.*'s calculation eliminates many of the kinematical approximations employed in the previous calculations.

Given these developments based on the phenomenological Lagrangians, we consider it important to examine the significance of these phenomenological Lagrangians in chiral perturbation theory (χPT) [14,15] which in general serves as a guiding principle for low-energy hadron dynamics. In the present work we shall describe an attempt at relating the traditional phenomenological approaches to χPT. The fact that χPT accounts for and improves the results of the current algebra also makes it a natural framework for studying threshold pion production. Furthermore, in this low-energy regime, it is natural to employ the heavy-fermion formalism (HFF) [16]. The HFF has an additional advantage of allowing easy comparison with Eqs. (2) and (3).

It should be mentioned, however, that the application of χPT to nuclei involves some subtlety. As emphasized by Weinberg [17], naive chiral counting fails for a nucleus, which is a loosely bound many-body system. This is because purely nucleonic intermediate states occurring in a nucleus can have very low excitation energies, which spoils the ordinary chiral counting. To avoid this difficulty, one must first classify diagrams appearing in perturbation series into irreducible and reducible diagrams, according to whether or not a diagram is free from purely nucleonic intermediate states. Thus, in an irreducible diagram, every intermediate state contains at least one meson. The χPT can be safely applied to the irreducible diagrams. The contribution of all the irreducible diagrams (up to a specified chiral order) is then to be used as an effective operator acting on the nucleonic Hilbert space. This second step allows us to incorporate the contributions of the reducible diagrams. We may refer to this two-step procedure as the *nuclear chiral perturbation theory* (nuclear χPT). This method was first applied by Weinberg [17] to chiral-perturbation-theoretical derivation of the nucleon-nucleon interactions and subsequently used by van Kolck *et al.* [18]. Park, Min, and Rho (PMR) [19] applied the nuclear χPT to meson exchange currents in nuclei. The success of the nuclear χPT in describing the exchange currents for the electromagnetic and weak interactions is well known [19–21]. The present paper is in the spirit of the work of PMR.

This article is organized as follows: In the next section we define our pion field and the chiral counting procedure. Then in Sec. III we present the two lowest order Lagrangians, discuss their connection to the early works on this reaction and determine within certain approximations the numerical values of the effective pion rescattering vertex strength, $\kappa_{\rm th}$. In Sec. IV we briefly discuss the connection between the transition matrix for this reaction and the χPT calculated amplitude. In Sec. V we present necessary loop corrections to the Born term, and in Sec. VI we calculate the cross section and discuss the various approximations and the uncertainties of the low energy constants in χPT. Finally in Sec. VII, after discussing some higher chiral order diagrams, we present our main conclusions.

A work very similar in spirit to ours has recently been completed by Cohen *et al.* [22].

II. CHIRAL PERTURBATION THEORY

The effective chiral Lagrangian $\mathscr{L}_{\rm ch}$ involves an SU(2) matrix $U(x)$ that is nonlinearly related to the pion field and that has standard chiral transformation properties [23]. An example is [24]

$$U(x)=\sqrt{1-[\boldsymbol{\pi}(x)/f_\pi]^2}+i\boldsymbol{\tau}\cdot\boldsymbol{\pi}(x)/f_\pi . \tag{5}$$

In the meson sector, the sum of chiral-invariant monomials constructed from $U(x)$ and its derivatives constitutes the chiral-symmetric part of $\mathscr{L}_{\rm ch}$. Furthermore, one can construct systematically the symmetry-breaking part of $\mathscr{L}_{\rm ch}$ with the use of a mass matrix $\mathscr{M}$ the chiral transformation of which is dictated by that of the quark mass term in the QCD Lagrangian. To each term appearing in $\mathscr{L}_{\rm ch}$ one can assign a chiral order index $\bar{\nu}$ defined by

$$\bar{\nu}\equiv d-2, \tag{6}$$

where d is the summed power of the derivative and the pion mass involved in this term. A low energy phenomenon is characterized by a generic pion momentum Q, which is small compared to the chiral scale $\Lambda\sim$ 1 GeV. It can be shown that the contribution of a term of chiral order $\bar{\nu}$ carry a factor $(\tilde{Q}/\Lambda)^{\bar{\nu}}$, where $\tilde{Q}$ represents either Q or the pion mass m_π. This suggests the possibility of describing low-energy phenomena in terms of $\mathscr{L}_{\rm ch}$ that contains only a manageably limited number of terms of low chiral order. This is the basic idea of χPT.

The heavy fermion formalism (HFF) [16] allows us to easily extend χPT to the meson-nucleon system. In HFF, the ordinary Dirac field ψ describing the nucleon, is replaced by the heavy nucleon field $N(x)$ and the accompanying "small component field" $n(x)$ through the transformation

$$\psi(x)=\exp(-im_N v\cdot x)[N(x)+n(x)] \tag{7}$$

with

$$\not{v}N=N, \quad \not{v}n=-n, \tag{8}$$

where the four-velocity v_μ is assumed to be almost static, i.e., $v_\mu\approx(1,0,0,0)$ [25]. Elimination of $n(x)$ in favor of $N(x)$ leads to expansion in ∂_μ/m_N. Since $m_N\approx$ 1 GeV $\approx\Lambda$, an expansion in ∂_μ/m_N may be treated like an expansion in ∂_μ/Λ. $\mathscr{L}_{\rm ch}$ in HFF consists of chiral symmetric monomials constructed from $U(x)$, $N(x)$ and their derivatives and of symmetry-breaking terms involving $\mathscr{M}$. The chiral order $\bar{\nu}$ in HFF is defined by

$$\bar{\nu}\equiv d+n/2-2, \tag{9}$$

where d is, as before, the summed power of the derivative and the pion mass, while n is the number of nucleon fields involved in a given term. As before, a term in $\mathscr{L}_{\rm ch}$ with chiral order $\bar{\nu}$ can be shown to carry a factor $(\tilde{Q}/\Lambda)^{\bar{\nu}}\ll 1$. In what follows, $\bar{\nu}$ stands for the chiral order defined in Eq. (9).

In addition to the chiral order index $\bar{\nu}$ defined for each term in $\mathscr{L}_{\rm ch}$, we assign a chiral order index ν for each irreducible Feynman diagram appearing in the chiral perturbation series for a multifermion system [17]. Its definition is

$$\nu=4-E_N-2C+2L+\sum_i \bar{\nu}_i , \tag{10}$$

where E_N is the number of nucleons in the Feynman diagram, L the number of loops, and C the number of disconnected parts of the diagram. The sum over i runs over all the vertices in the Feynman graph, and $\bar{\nu}_i$ is the chiral order of each vertex. One can show [17] that an irreducible diagram of chiral order ν carries a factor $(\tilde{Q}/\Lambda)^{\nu}\ll 1$.

In the literature the term "effective Lagrangian" (or "effective Hamiltonian") is often used to imply that that Lagrangian (or Hamiltonian) is only meant for calculating tree diagrams. The Hamiltonians given in Eqs. (2) and (3) are regarded as effective Hamiltonians of this type. We must note, however, that the effective Lagrangian in χPT has a different meaning. Not only can $\mathscr{L}_{\rm ch}$ be used beyond tree approximation but, in fact, a consistent chiral counting even demands inclusion of every loop diagram whose chiral order ν is lower than or equal to the chiral order of interest. As will be discussed below, for a consistent χPT treatment of the problem at hand, we therefore need to consider loop corrections. However, since the inclusion of the loop corrections is rather technical, we find it useful to first concentrate on the tree-diagram contributions. This simplification allows us to understand the basic aspects of the relation between the contributions from χPT and the phenomenological Hamiltonians, Eqs. (2) and (3). Therefore, in the next two sections (III and IV) we limit our discussion to tree diagrams. A more elaborate treatment including loop corrections will be described in Sec. V.

III. TREE DIAGRAM CONSIDERATIONS

In order to produce the one-body and two-body diagrams depicted in Figs. 1(a) and 1(b), we minimally need (see below) terms with $\bar{\nu}=1$ and 2 in $\mathscr{L}_{\rm ch}$. We therefore work with

$$\mathscr{L}_{\rm ch}=\mathscr{L}^{(0)}+\mathscr{L}^{(1)}, \tag{11}$$

where $\mathscr{L}^{(\bar{\nu})}$ represents terms of chiral order $\bar{\nu}$. Their explicit forms are [15,26]

$$\mathscr{L}^{(0)}=\frac{f_\pi^2}{4}\,\mathrm{Tr}[\partial_\mu U^\dagger\partial^\mu U+m_\pi^2(U^\dagger+U-2)] \tag{12a}$$

$$+\bar{N}(iv\cdot D+g_A S\cdot u)N \tag{12b}$$

$$-\frac{1}{2}\sum_A C_A(\bar{N}\Gamma_A N)^2, \tag{12c}$$

$$\mathscr{L}^{(1)}=-\frac{ig_A}{2m_N}\bar{N}\{S\cdot D,v\cdot u\}N \tag{12d}$$

$$+2c_1 m_\pi^2\bar{N}N\,\mathrm{Tr}(U+U^\dagger-2) \tag{12e}$$

$$+\left(c_2-\frac{g_A^2}{8m_N}\right)\bar{N}(v\cdot u)^2N+c_3\bar{N}u\cdot uN \tag{12f}$$

$$-\frac{c_9}{2m_N}(\bar{N}N)(\bar{N}iS\cdot uN) \tag{12g}$$

$$-\frac{c_{10}}{2m_N}(\bar{N}S^\mu N)(\bar{N}iu_\mu N). \tag{12h}$$

In the above

$$\xi\equiv\sqrt{U(x)}, \tag{13}$$

$$u_\mu\equiv i(\xi^\dagger\partial_\mu\xi-\xi\partial_\mu\xi^\dagger), \tag{14}$$

$$D_\mu N\equiv(\partial_\mu+\tfrac{1}{2}[\xi^\dagger,\partial_\mu\xi])N, \tag{15}$$

and S_μ is the covariant spin operator defined by

$$S_\mu\equiv\tfrac{1}{4}\gamma_5[\not{v},\gamma_\mu]. \tag{16}$$

In $\mathscr{L}^{(1)}$ above we have retained only terms of direct relevance for our discussion. The coupling constants c_1,c_2 and c_3 can be fixed from phenomenology [15]. They are related to the pion-nucleon σ term, $\sigma_{\pi N}(t)\sim\langle p'|\bar{m}(\bar{u}u+\bar{d}d)|p\rangle$ [$\bar{m}$=average mass of the light quarks, $t=(p'-p)^2$], the axial polarizability α_A and the isospin-even πN s-wave scattering length $a^+\equiv\frac{1}{3}(a_{1/2}+2a_{3/2})\approx-0.008m_\pi^{-1}$ [7]. (The explicit expressions will be given below.) It should be noted that in HFF, a part of the term in $\mathscr{L}^{(1)}$ with the coefficient $(c_2-g_A^2/8m_N)$, namely the $-g_A^2/8m_N$ piece, represents the s-wave π-N scattering contribution, which in a traditional calculation is obtained from the crossed Born term.

The four-Fermi nonderivative contact terms in Eq. (12) were introduced by Weinberg [17] and further investigated in two- and three-nucleon systems by van Kolck *et al.* [18]. Although these terms are important in the chiral perturbative derivation of the nucleon-nucleon interactions [17,18], they do not play a major role in the following discussion of the threshold $pp\to pp\pi^0$ reaction. We therefore temporarily ignore these four-fermion terms and come back to a discussion of these terms in the last section.

The Lagrangian (11) leads to the pion-nucleon interaction Hamiltonian

$$\mathscr{H}_{\rm int}=\mathscr{H}_{\rm int}^{(0)}+\mathscr{H}_{\rm int}^{(1)}, \tag{17}$$

where

$$\mathscr{H}_{\rm int}^{(0)}=\frac{g_A}{2f_\pi}\bar{N}[\boldsymbol{\sigma}\cdot\nabla(\boldsymbol{\tau}\cdot\boldsymbol{\pi})]N+\frac{1}{4f_\pi^2}\bar{N}\boldsymbol{\tau}\cdot\boldsymbol{\pi}\times\dot{\boldsymbol{\pi}}N, \tag{18a}$$

$$\mathscr{H}_{\rm int}^{(1)}=\frac{-ig_A}{4m_N f_\pi}\bar{N}\{\boldsymbol{\sigma}\cdot\nabla,\boldsymbol{\tau}\cdot\dot{\boldsymbol{\pi}}\}N+\frac{1}{f_\pi^2}\left[2c_1m_\pi^2\pi^2-\left(c_2-\frac{g_A^2}{8m_N}\right)\dot{\pi}^2-c_3(\partial\pi)^2\right]\bar{N}N. \tag{18b}$$

Here $\mathscr{H}_{\rm int}^{(\bar{\nu})}$ represents the term of chiral order $\bar{\nu}$.

We now compare $\mathscr{H}_{\rm int}$ resulting from χPT, Eq. (17) with the phenomenological effective Hamiltonian $\mathscr{H}_0+\mathscr{H}_1$, Eqs. (2) and (3). (The reader is reminded that the chiral index $\bar{\nu}$ should not be confused with the suffix appearing in $\mathscr{H}_0$ and $\mathscr{H}_1$.) Regarding the πNN vertices, we note that the first term in $\mathscr{H}^{(0)}$ and the first term in $\mathscr{H}^{(1)}$ exactly correspond to the first and second terms, respectively, in $\mathscr{H}_0$. Thus the so-called Galilean-invariance term naturally arises as a $1/m_N$ correction term in HFF. As for the $\pi\pi NN$ vertices, we can associate the second term in $\mathscr{H}_{\rm int}^{(0)}$ to the λ_2 term in $\mathscr{H}_1$, and second term in $\mathscr{H}_{\rm int}^{(1)}$ to the λ_1 term in $\mathscr{H}_1$. This suggests the following identifications:

$$4\pi\frac{\lambda_2}{m_\pi^2}=\frac{1}{4f_\pi^2} \tag{19}$$

and

$$4\pi\lambda_1/m_\pi=\frac{m_\pi^2}{f_\pi^2}\left[2c_1-\left(c_2-\frac{g_A^2}{8m_N}\right)\frac{\omega_q\omega_k}{m_\pi^2}-c_3\frac{q\cdot k}{m_\pi^2}\right]\equiv\kappa(k,q). \tag{20}$$

In Eq. (20), $q=(\omega_q,\mathbf{q})$ and $k=(\omega_k,\mathbf{k})$ stand for the four-momenta of the exchanged-and final pions, respectively; see Fig. 1(b). Since, as already discussed, the λ_2 term is not important for our purposes, we shall concentrate on the λ_1 term. The best available estimates of the coefficients c_i (i=1-3) can be found in Refs. [15,27], which give

$$c_1=-\frac{1}{4m_\pi^2}\left[\sigma_{\pi N}(0)+\frac{9g_A^2m_\pi^3}{64\pi f_\pi^2}\right] \tag{21a}$$

$$=-0.87\pm0.11\ \mathrm{GeV}^{-1}, \tag{21b}$$

$$c_3=-\frac{f_\pi^2}{2}\left[\alpha_A+\frac{g_A^2m_\pi}{8f_\pi^2}\left(\frac{77}{48}+g_A^2\right)\right] \tag{21c}$$

$$=-5.25\pm0.22\ \mathrm{GeV}^{-1}, \tag{21d}$$

$$c_2=\frac{f_\pi^2}{2m_\pi^2}\left[4\pi\left(1+\frac{m_\pi}{m_N}\right)a^+-\frac{3g_A^2m_\pi^3}{64\pi f_\pi^4}\right] \tag{21e}$$

$$+2c_1-c_3+\frac{g_A^2}{8m_N} \tag{21f}$$

$$=3.34\pm0.27\ \mathrm{GeV}^{-1}. \tag{21g}$$

The numerical results are based on the experimental values: $\sigma_{\pi N}(0)=45\pm8$ MeV [28], $\alpha_A=2.28\pm0.10m_\pi^{-3}$ [7], and $a^+=(-0.83\pm0.38)\times10^{-2}m_\pi^{-1}$ [29]. We shall show in Sec. VI that the uncertainties in the numerical value for c_2 might be larger than quoted in Eq. (21g). In fact, the terms in Eqs. (21b)–(21g) proportional to the $(g_A/f_\pi)^2$ are $O[(m_\pi/\Lambda)^3]$ corrections arising from finite terms of $\mathscr{L}^{(2)}$. However, since the present section is just an introduction to a later systematic treatment, this inconsistency in ''accuracy'' will be ignored for the moment.

Now, for *on-shell* low energy pion-nucleon scattering, i.e., $k\sim q\sim(m_\pi,\mathbf{0})$, we equate

$$4\pi\lambda_1/m_\pi=\kappa_0\equiv\kappa[k=(m_\pi,\mathbf{0}),q=(m_\pi,\mathbf{0})], \tag{22}$$

where

$$\kappa_0=\frac{m_\pi^2}{f_\pi^2}\left(\tilde{c}+\frac{g_A^2}{8m_N}\right), \tag{23}$$

$$\tilde{c}\equiv2c_1-c_2-c_3. \tag{24}$$

From Eq. (21) we have

$$\tilde{c}=-\frac{f_\pi^2}{2m_\pi^2}\left[4\pi\left(1+\frac{m_\pi}{m_N}\right)a^+-\frac{3g_A^2m_\pi^3}{64\pi f_\pi^4}\right]-\frac{g_A^2}{8m_N}, \tag{25}$$

which results in

$$\kappa_0=-2\pi\left(1+\frac{m_\pi}{m_N}\right)a^++\frac{3g_A^2}{128\pi}\frac{m_\pi^3}{f_\pi^4}. \tag{26}$$

The above cited empirical value for a^+ leads to

$$\tilde{c}=(0.59\pm0.09)\ \ \mathrm{GeV}^{-1}, \tag{27}$$

$$\kappa_0=(0.87\pm0.20)\ \ \mathrm{GeV}^{-1}. \tag{28}$$

We now interpret these results in terms of λ_1 of Eq. (3). Conventionally, λ_1 is determined from Eq. (4a) which is the first term in Eq. (26). Thus

$$\frac{4\pi\lambda_1}{m_\pi}=-2\pi\left(1+\frac{m_\pi}{m_N}\right)a^+, \tag{29}$$

which gives

$$\frac{4\pi\lambda_1}{m_\pi}=(0.43\pm0.20)\ \ \mathrm{GeV}^{-1}, \tag{30}$$

or $\lambda_1=0.005\pm0.002$. This is the ''standard value'' used in the literature [7,30]. On the other hand, the right-hand side of Eq. (22) based on χPT gives from Eq. (28)

$$\frac{4\pi\lambda_1}{m_\pi}=(0.87\pm0.20)\ \ \mathrm{GeV}^{-1}, \tag{31}$$

which is about twice as large as the conventional value. This means the second term in Eq. (26) is almost as large as the first term. Thus χPT leads to a substantial modification of the commonly used formula, Eq. (4a) or Eq. (29). This large ''higher chiral order'' corrections due to $\mathscr{L}^{(2)}$ [the term proportional to $(g_A/f_\pi)^2$ in Eq. (26)] indicates that χPT does not converge very rapidly in this particular case. This apparent lack of convergence is probably due to the fact that the first terms in expansion, the π-N isoscalar scattering length a^+, is exceptionally small.

To develop further the connection between the traditional and the χPT approaches, we return to a discussion of Eq. (20). Obviously, the constant λ_1 cannot be fully identified with $\kappa(k,q)$ which depends on the momenta q and k. In fact, the momentum dependence of $\kappa(k,q)$ should play a significant role in describing the physical pion-nucleon elastic scattering process where $\omega_q=\sqrt{m_\pi^2+\mathbf{q}^2}$, $\omega_k=\sqrt{m_\pi^2+\mathbf{k}^2}$. An additional crucial point in the present context is that, in the rescattering diagram Fig. 1(b), the exchanged pion can be far off-shell, and therefore the q and k dependence in $\kappa(k,q)$ may play an even more pronounced role. As an illustration, let us consider again the *typical threshold kinematics* discussed in the introduction: $q\sim(m_\pi,\mathbf{0})$ and $k\sim(\frac{1}{2}m_\pi,\sqrt{m_\pi m_N})$. If we denote by κ_{th} the value of $\kappa(k,q)$ [Eq. (20)] corresponding to the *typical threshold kinematics*, we have

$$\kappa_{\mathrm{th}}=\frac{m_\pi^2}{f_\pi^2}\left[2c_1-\frac{1}{2}\left(c_2-\frac{g_A^2}{8m_N}\right)-\frac{c_3}{2}\right]. \tag{32}$$

The use of the central values for the coupling constants c_1,c_2 and c_3 leads to

$$4\pi\lambda_1/m_\pi=\kappa_{\mathrm{th}}\sim-1.5\ \ \mathrm{GeV}^{-1}. \tag{33}$$

Thus the strength of the s-wave pion-nucleon interaction here is much stronger than the on-shell cases, see Eqs. (30) and (31), and the sign of the off-shell coupling strength is *opposite* to the on-shell cases. The first feature is qualitatively in line with the observation of Hernández and Oset [11] that the rescattering term should be larger than previously considered. However, the sign of the typical off-shell coupling in our case [Eq. (33)] is opposite to the one used in Ref. [11]. As will be discussed later, this flip of the sign drastically changes the pattern of interplay between the Born and rescattering terms. We must emphasize that the off-shell enhancement depends strongly on the values of c_1, c_2, and c_3, which, as discussed in Refs. [15,27], are not known very accurately. It is therefore important to examine to what extent the existing large ambiguities in c_1, c_2, and c_3 affect the off-shell enhancement of the $pp\to pp\pi^0$ reaction. We shall address this question in Sec. VI.

IV. TRANSITION OPERATORS FOR $pp\to pp\pi^0$

As explained earlier, in the nuclear χPT we first use χPT to calculate the contributions of the irreducible diagrams. Let $\mathscr{T}$ represent the contributions of all irreducible diagrams (up to a specified chiral order ν) for the $pp\to pp\pi^0$ process. Then we use $\mathscr{T}$ as an effective transition operator in the Hilbert space of nuclear wave functions. Consequently, the two-nucleon transition matrix element T for the $pp\to pp\pi^0$ process is given by

$$T=\langle\Phi_f|\mathscr{T}|\Phi_i\rangle, \tag{34}$$

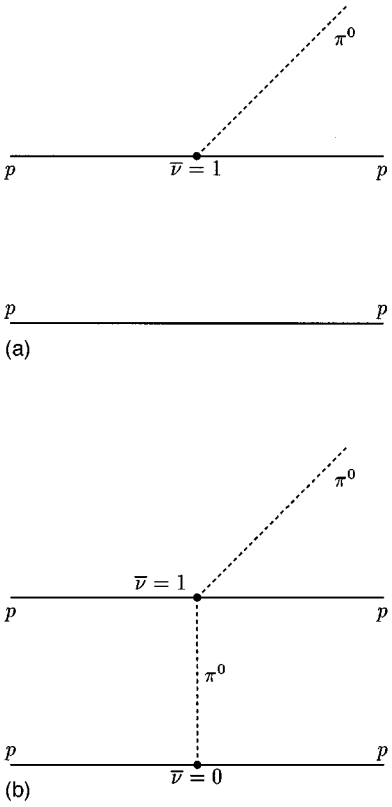

FIG. 2. Tree graphs: the Born term (a) ($\nu=-1$) and the pion rescattering term (b) ($\nu=1$).

where $|\Phi_i\rangle$ ($|\Phi_f\rangle$) is the initial (final) two-nucleon state distorted by the initial-state (final-state) interaction. These distorted waves should be obtained by solving the Schrödinger equation with nucleon-nucleon interactions generated by irreducible diagrams pertinent to nucleon-nucleon scattering, thereby incorporating an infinite number of ''reducible'' ladder diagrams. In this section we concentrate on the derivation of the transition operator $\mathscr{T}$, relegating the discussion of T and Eq. (34) to Sec. VI.

We decompose $\mathscr{T}$ as

$$\mathscr{T}=\sum_{\nu}\mathscr{T}^{(\nu)}, \tag{35}$$

where $\mathscr{T}^{(\nu)}$ represents the contribution from Feynman diagrams of chiral order ν, as defined in Eq. (10). The lowest value of ν occurs for the Born term shown in Fig. 2(a). For s-wave π production at threshold the $NN\pi$ vertex with $\bar{\nu}=0$, the first term in Eq. (17), cannot contribute; hence the lowest $\bar{\nu}$ for $NN\pi$ vertex involving an external pion must be $\bar{\nu}=1$. The first term in Eq. (18b) provides this vertex. According to Eq. (10), the chiral order of Fig. 2(a) is given by $\nu=4-2-2\times2+2\times0+1=-1$. As can be checked easily, there are no diagrams with $\nu=0$ since in the rescattering diagram, Fig. 2(b), the second term in Eq. (18a), which gives the $NN\pi\pi$ vertex with $\bar{\nu}=0$, is not operative here due to the isospin selection rule. The rescattering diagram in Fig. 2(b) with the indicated value of $\bar{\nu}$ at each vertex contributes to $\mathscr{T}^{(\nu=1)}$. It should be noted that because of the $-2C$ term in the chiral counting expression, Eq. (10), exchange-current-type diagrams such as Fig. 2(b) give higher values of ν. In this work we truncate the calculation of the transition operator $\mathscr{T}$ at $\nu=1$. Thus

$$\mathscr{T}=\mathscr{T}^{(-1)}+\mathscr{T}^{(1)}. \tag{36}$$

The above enumeration is, as briefly discussed in Sec. III, far from complete because loop diagrams and counter terms and finite terms from $\mathscr{L}^{(2)}$ have been left out. In Fig. 3 we show the loop corrections to the Born term [Fig. 2(a)]. The diagrams in Fig. 3 all have $\nu=1$ and hence are of the same chiral order as the leading order rescattering diagram, Fig. 2(b). As discussed earlier, for the $pp\to pp\pi^0$ reaction at threshold the contribution of the Born term is numerically suppressed so that the rescattering diagram, which is formally of higher chiral order by two units of ν, plays an essential role. This implies that a meaningful and consistent χPT calculation of this reaction must include the loop corrections to the leading-order Born term. However, we continue to postpone the discussion of loop corrections to the next section.

The tree diagrams contributing to Eq. (36), Figs. 2(a) and 2(b), are as follows. The Born term, Fig. 2(a), contributes to

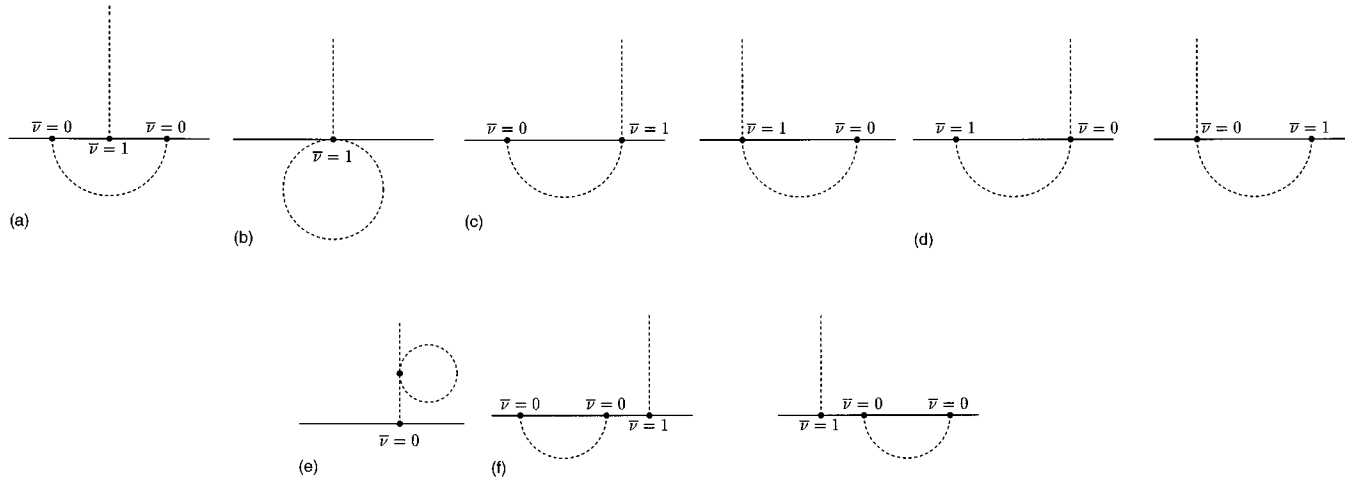

FIG. 3. Loop corrections to the Born term.

$\mathscr{T}^{(-1)}$ and the rescattering term, Fig. 2(b), contributes to $\mathscr{T}^{(1)}$. These contributions are given, respectively, by

$$\mathscr{T}^{\rm Born}_{-1}=\frac{g_A}{4m_N f_\pi}\omega_q\sum_{i=1,2}\boldsymbol{\sigma}_i\cdot(\boldsymbol{p}_i'+\boldsymbol{p}_i)\tau_i^0, \tag{37a}$$

$$\mathscr{T}^{\rm res}_{+1}=-\frac{g_A}{f_\pi}\sum_{i=1,2}\kappa(k_i,q)\frac{\boldsymbol{\sigma}_i\cdot\boldsymbol{k}_i\tau_i^0}{k_i^2-m_\pi^2+i\varepsilon}, \tag{37b}$$

where $\boldsymbol{p}_i$ and $\boldsymbol{p}'_i$ $(i=1,2)$ denote the initial and final momenta of the ith proton, $\boldsymbol{k}_i\equiv\boldsymbol{p}_i-\boldsymbol{p}'_i$; and $\kappa(k_i,q)$ is as defined in Eq. (20).

V. LOOP DIAGRAMS

We have emphasized above that the loop corrections to the Born diagram, Fig. 2(a), which has chiral order $\nu=-1$, are of the same chiral order $\nu=1$ as the two-body pion rescattering process, Fig. 2(b). These loop corrections therefore must be included in a consistent $\nu=1$ calculation.

For our present purposes it is not necessary to go into a general discussion of the renormalization of the parameters in $\mathscr{L}_{\rm ch}$. Instead we concentrate on an estimation of the size of the finite loop corrections to the specific tree level terms shown in Fig. 2. This will be done by applying standard Feynman rules and using dimensional regularization [15]. Specifically, we need only consider the loop corrections to the single $\pi^0 NN$ vertex in the s-wave channel:

$$\mathscr{T}^{\rm Born}_{-1}+\mathscr{T}^{\rm corr}_{+1}=\left(-\frac{g_A}{2m_N f_\pi}\right)\sum_{i=1,2}[S_i\cdot(p_i\prime+p_i)](v\cdot q)\tau_i^0\mathscr{V}, \tag{38}$$

where $S_i=(0,\frac{1}{2}\boldsymbol{\sigma}_i)$ is the spin of the ith proton and $\mathscr{V}$ is the amplitude to be calculated. For the Born term [Fig. 2(a)] itself we have

$$\mathscr{V}_{2a}=1 \tag{39}$$

given by Eq. (37a). The loop diagrams [Figs. 3(a)–3(f)], which renormalize the s-wave Born term, give the following contributions:

$$\mathscr{V}_{3a}=\frac{1}{4}\left(\frac{g_A}{f_\pi}\right)^2\frac{J_2(vp')-J_2(vp)}{vq}, \tag{40a}$$

$$\mathscr{V}_{3b}=-\frac{\Delta_\pi}{2f_\pi^2}, \tag{40b}$$

$$\mathscr{V}_{3c}=\frac{1}{2f_\pi^2}\frac{J_2(vp')-J_2(vp)}{vq}, \tag{40c}$$

$$\mathscr{V}_{3d}=\frac{1}{2f_\pi^2}\left(3\Delta_\pi+[(vp)J_0(vp)+(vp')J_0(vp')]+\frac{(vp)^2J_0(vp)-(vp')^2J_0(vp')}{vq}\right). \tag{40d}$$

Here we have adopted the notations of Ref. [15]. Thus

$$\Delta_\pi\equiv\frac{1}{i}\int\frac{d^dl}{(2\pi)^d}\frac{1}{m_\pi^2-l^2}=m_\pi^{d-2}(4\pi)^{d/2}\Gamma\left(1-\frac{d}{2}\right) \tag{41}$$

$$=2m_\pi^2\left(L+\frac{1}{16\pi^2}\ln\frac{m_\pi}{\lambda}\right), \tag{42}$$

where the divergence is included in

$$L=\frac{\lambda^{d-4}}{16\pi^2}\left[\frac{1}{d-4}+\frac{1}{2}(\gamma_E-1-\ln 4\pi)\right]. \tag{43}$$

In this expression λ denotes the dimensional regularization scale and $\gamma_E=0.557\,215$. Furthermore, J_0 and J_2 in Eqs. (40) are defined by

$$J_0(\omega)=-4L\omega+\frac{\omega}{8\pi^2}\left(1-2\ln\frac{m_\pi}{\lambda}\right)-\frac{1}{4\pi^2}\sqrt{m_\pi^2-\omega^2}\arccos\left(\frac{-\omega}{m_\pi}\right) \tag{44}$$

and

$$J_2(\omega)=\frac{1}{d-1}[(m_\pi^2-\omega^2)J_0(\omega)-\omega\Delta_\pi]. \tag{45}$$

The two contributions to $\mathscr{V}$, Eqs. (40c) and (40d), originate from two different combinations of terms in Eqs. (18). To calculate Eq. (40c), the second term in Eq. (18a) and the first term in Eq. (18b) are used at the vertices, whereas Eq. (40d) is calculated using the first term of Eq. (18a) and the second term of Eq. (18b).

The standard renormalization consists in the following procedure.

(1) The loop contributions to $\mathscr{V}$ are separated into a divergent part, which we take to be proportional to L of Eq. (43) and which contains a pole at $d=4$, and a finite part:

$$\mathscr{V}_3=\mathscr{V}_3|^{\infty}+\mathscr{V}_3|^{\rm finite}. \tag{46}$$

(2) Local counter terms, which are of the same chiral order as the loop diagrams, are added. In our case these counterterms must come from the Lagrangian $\mathscr{L}^{(3)}$,

$$\mathscr{L}^{(3)}=\frac{1}{(4\pi f_\pi)^2}\sum_i D_i\bar{N}O_iN, \tag{47}$$

to give two-nucleon diagrams with $\nu=1$. The unknown constants D_i are then written as a sum of a finite and an infinite part

$$D_i=D_i|^{\rm finite}(\lambda)+(4\pi)^2\delta_i L. \tag{48}$$

The constants δ_i are determined by requiring that the infinite part of D_i cancel the divergent part $\mathscr{V}_3|^{\infty}$. The remaining finite contributions which should be added to the Born term via Eq. (38), are

$$\mathscr{V}_{\rm loop}=\mathscr{V}_3|^{\rm finite}+\mathscr{V}_{\rm c.t.}|^{\rm finite}. \tag{49}$$

The amplitude $\mathscr{V}_3$ contains energy-independent and energy-dependent parts, as can be seen in Eq. (40). The energy-

independent part can be absorbed in the renormalization of the following physical parameters: the pion wave function renormalization factor Z_π [Fig. 3(e)], the nucleon mass m_N and the nucleon wave function renormalization factor Z_N [(Fig. 3(f)], as well as the axial coupling constant g_A [Figs. 3(a), 3(b), 3(e), 3(f)]. For the evaluation of the energy-dependent part we use the *typical threshold kinematics*: $vq=m_\pi$, $vp_1=m_\pi$, $vp_2=0$. Putting these values into the corresponding terms in Eq. (40), we obtain as the total contribution of the diagrams in Fig. 3

$$\mathscr{V}_3|^{\text{finite}} \approx 0.1. \tag{50}$$

Thus $\mathscr{V}_3|^{\text{finite}}$ amounts to 10% of the Born term [Fig. 2(a)]. In addition we have finite contributions from the counterterms of $\mathscr{L}^{(3)}$, $\mathscr{V}_{\text{c.t.}}|^{\text{finite}}$. We note that only very few of the low energy constants in the counterterms $D_i|^{\text{finite}}(\lambda)$ are known [15]. Some of the low energy constants in $\mathscr{L}^{(2)}$, $B_i|^{\text{finite}}(\lambda)$ have been estimated in Ref. [15] assuming Δ resonance saturation. The result indicates $B_i|^{\text{finite}}(\lambda) \approx O(0.1)$. For an estimate of the low energy constants $D_i|^{\text{finite}}(\lambda)$ in $\mathscr{L}^{(3)}$ it seems reasonable to assume that they are of the same order of magnitude as the $B_i|^{\text{finite}}(\lambda)$ in $\mathscr{L}^{(2)}$. To be conservative let us assume $D_i|^{\text{finite}}(\lambda) \approx O(1)$; then we expect $\mathscr{V}_{\text{c.t.}}|^{\text{finite}} \approx 0.1$. It is clear that, if those coefficients were ''unreasonably large,'' the convergence of the whole chiral series would be destroyed.

Altogether, after renormalization the total contributions from the loop terms are expected to amount to at most 20% of the Born term. This is not a completely negligible contribution in the present context because, as will be discussed in the next section, there can be a significant cancellation between the Born and the rescattering terms. Nevertheless, since our present treatment involves other larger uncertainties, we will neglect the renormalization of the Born term and henceforth concentrate on the bare Born term [Fig. 2(a)] and the rescattering term [Fig. 2(b)].

VI. CALCULATION OF THE TWO-NUCLEON TRANSITION MATRIX

We derived in Sec. IV the effective transition operator $\mathscr{T}$ arising from the tree diagrams and, in Sec. V, we estimated the additional contributions due to the loop corrections and presented an argument for ignoring the loop corrections in this work. These considerations lead to the HFF expression of $\mathscr{T}$ up to order $\nu = 1$, given in Eqs. (36) and (37), and this $\mathscr{T}$ is to be used in Eq. (34) to obtain the two-nucleon transition matrix T.

A formally ''consistent'' treatment of Eq. (34) would consist in using for $|\Phi_i\rangle$ and $|\Phi_f\rangle$ two-nucleon wave functions generated by irreducible diagrams of order up to $\nu=1$. A problem in this ''consistent'' χPT approach is that the intermediate two-nucleon propagators in Fig. 1 can be significantly off-mass-shell, which creates a difficulty in any χPT calculation. Another more practical problem is that, if we include the initial and final two-nucleon (N-N) interactions in diagrams up to chiral order $\nu=1$, these N-N interactions are not realistic enough to reproduce the known N-N observables. A pragmatic remedy for these problems is to use a phenomenological N-N potential to generate the distorted N-N wave functions. Park, Min, and Rho [21] used this hybrid approach to study the exchange-current in the $n+p\to\gamma+d$ reaction and at least, for the low-momentum transfer process studied in Ref. [21], the hybrid method is known to work extremely well.

Apart from the above-mentioned problem, there is a delicate aspect in the derivation of an effective two-body operator from a given Feynman diagram. Ordinarily, one works with **r**-space transition operators acting on **r**-representation wave functions, for the nuclear wave functions are commonly given in this representation. To this end, a Feynman amplitude which is most conveniently given in momentum space, is Fourier transformed into the **r** representation. This method works best for low momentum transfer processes which have substantial transition amplitudes for on-shell initial and final plane-wave states. However, the $pp\to pp\pi^0$ reaction at threshold does not belong to this category. For this reaction it is essential to recognize that the nucleon lines that appear as external lines in Fig. 2 are in fact internal lines in larger diagrams illustrated in Fig. 1. These internal lines can be far off-shell due to the initial- and final-state interactions. Indeed without this off-shell kinematics, the Born term [Fig. 2(a)] would not contribute at all. In the conventional approach, however, one ignores this feature in deriving $\mathscr{T}$ in coordinate representation. For example, in Fourier transforming an operator of the type of $\mathscr{T}^{\text{res}}_{+1}$, Eq. (37b), even though $\boldsymbol{p}_i$ and $\boldsymbol{p}_i'$ in Eq. (37b) in fact can be anything due to momentum transfers caused by the initial and final N-N interactions, it is a common practice to keep the energy of the propagating pion fixed at the value determined by the asymptotic energies of the nucleons. Hanhart *et al.* [13] made a critical study of the consequences of avoiding these kinematical approximations. They worked directly with the two-nucleon wave functions in momentum representation. In the present work we do not attempt at detailed momentum-space calculations and simply use the ''conventional'' Fourier transform method. Because of this and a few other approximations adopted, the numerical work presented here is admittedly of exploratory nature. Nonetheless, as we shall show, our semiquantitative study of T based on the chiral-theoretically motived transition operator $\mathscr{T}$ provide some valuable insight into the dynamics of the threshold $pp\to pp\pi^0$ reaction.

Let us denote the contribution of Fig. 2(b) for plane-wave initial and final states by $\langle p_1', p_2', q|\mathscr{T}^{(1)}|p_1, p_2\rangle$. We first calculate this matrix element for the *typical threshold kinematics* described earlier; for the meson variables, $q=(m_\pi, \mathbf{0})$ and $k=(m_\pi/2, \boldsymbol{k})$ with $|\mathbf{k}|=\sqrt{m_\pi m_N}$. Correspondingly, the coupling strength $\kappa(k,q)$ [Eq. (37b)] is taken to be $\kappa_{\text{th}}=-1.5\ \text{GeV}^{-1}$ [Eq. (33)]. Subsequently, by liberating the momentum variables $\mathbf{p}_1$, $\mathbf{p}_1'$, $\mathbf{p}_2$, and $\mathbf{p}_2'$ from the on-mass-shell conditions ($p_1^2=m_N^2, \ldots$), we treat $\langle p_1', p_2', q|\mathscr{T}^{(1)}|p_1, p_2\rangle$ as a function of $\mathbf{p}_1$, $\mathbf{p}_1'$, $\mathbf{p}_2$, and $\mathbf{p}_2'$. Let $T(\mathbf{p}_1', \mathbf{p}_2'; \mathbf{p}_1, \mathbf{p}_2)$ stand for this function. We still require momentum conservation at each vertex, which imposes the conditions $\mathbf{p}_1+\mathbf{p}_2=\mathbf{p}_1'+\mathbf{p}_2'+\mathbf{q}=0$, and $\mathbf{k}=\mathbf{p}_1'-\mathbf{p}_1=\mathbf{p}_2-\mathbf{p}_2'$. $T(\mathbf{p}_1', \mathbf{p}_2'; \mathbf{p}_1, \mathbf{p}_2)$ can be easily Fourier transformed to give $\mathscr{T}^{\text{res}}_{+1}$ in **r** representation. The simplified treatment described here, which is commonly used in the litera-

ture, shall be referred to as the *fixed kinematics approximation*.

Now, in the *fixed kinematics approximation*, $\mathscr{T}$ [Eqs. (36), (37)] is translated into differential operators acting on relative coordinate of the two-nucleon wave functions:

$$\tilde{\mathscr{T}}_{-1}^{\text{Born}} = \frac{g_A}{f_\pi}\frac{m_\pi}{m_N}\boldsymbol{\Sigma}\cdot\nabla_r, \tag{51a}$$

$$\tilde{\mathscr{T}}_{+1}^{\text{res}} = -\frac{2g_A}{f_\pi}\kappa_{\text{th}}\boldsymbol{\Sigma}\cdot\hat{\boldsymbol{r}}f'(r), \tag{51b}$$

where the derivative operator with subscript r is to act on the relative coordinate $\boldsymbol{r}$ between two protons, and $\boldsymbol{\Sigma}\equiv\frac{1}{2}(\boldsymbol{\sigma}_1-\boldsymbol{\sigma}_2)$. The trivial isospin operator τ_i^0 has been dropped. The Yukawa function $f(r)\equiv\exp(-\mu' r)/4\pi r$ is defined with the *effective* mass $\mu'=\sqrt{3}/2\, m_\pi$. We reemphasize that the simple Yukawa form $f(r)$ arises only when the *fixed kinematics approximation* just discussed is used.

From this point on, our calculation of T follows exactly the traditional pattern described in the literature. Thus T is evaluated by inserting the transition operators, $\tilde{\mathscr{T}}_{-1}^{\text{Born}}$ and $\tilde{\mathscr{T}}_{+1}^{\text{res}}$, Eq. (51), between the initial and final nuclear states

$$\begin{aligned}\phi_i(\boldsymbol{r}) &= (\sqrt{2}/pr)iu_{1,0}(r)e^{i\delta_{1,0}}(4\pi)^{1/2}|^{3,3}P_0\rangle,\\ \phi_f(\boldsymbol{r}) &= (1/p'r)u_{0,0}(r)e^{i\delta_{0,0}}(4\pi)^{1/2}|^{3,1}S_0\rangle,\end{aligned} \tag{52}$$

where p and p' are the asymptotic relative three-momenta of the initial and final two-proton systems. The wave functions are normalized as $u_{L,J}\overset{r\to\infty}{\to}\sin(pr-\frac{1}{2}\pi L+\delta_{L,J})$ with $\delta_{L,J}$ being the N-N scattering phase shifts. For simplicity, the Coulomb interactions between the two protons is ignored. (The Coulomb force is known to reduce the cross section up to 30% [4].) The explicit expression for the transition amplitude at threshold is obtained as

$$T(E_f) = 4\pi(g_A/f_\pi m_N m_\pi^{3/2})(J_{-1}^{\text{Born}}+J_{+1}^{\text{res}}). \tag{53}$$

Here, $E_f = E_{p'}+\boldsymbol{q}^2/2m_\pi$ is the kinetic energy of the final state, and

$$J_{-1}^{\text{Born}} = \lim_{p'\to 0}\frac{-m_\pi^2}{pp'}\int_0^\infty dr\; r^2\frac{u_{0,0}}{r}\left(\frac{d}{dr}+\frac{2}{r}\right)\frac{u_{1,0}}{r}, \tag{54a}$$

$$J_{+1}^{\text{res}} = \lim_{p'\to 0} 2\kappa_{\text{th}}\frac{m_\pi M_n}{pp'}\int_0^\infty dr\; u_{0,0}f'(r)u_{1,0}. \tag{54b}$$

The total cross section is obtained by multiplying the absolute square of the transition amplitude (averaged over the initial spins and summed over the final spins) with the appropriate phase space factor $\rho(E_f)$ and the flux factor $1/v$:

$$\sigma_{\text{tot}} = \frac{2\pi}{v}\int d\rho(E_f)|T(E_f)|^2. \tag{55}$$

For a rough estimation one may approximate the energy dependence of the transition matrix as [31]

$$|T(E_f)|^2 = \frac{|T(0)|^2}{1+p'^2a^2}, \tag{56}$$

TABLE I. J_{-1}^{Born} and J_{+1}^{res} for the threshold kinematics [Eqs. (54a),(54b)], calculated with the Hamada-Johnsotn (HJ) and Reid soft-core (RSC) potentials.

	HJ	RSC
J_{-1}^{Born}	-0.672	-0.515
J_{+1}^{res}	$+0.505$	$+0.413$

where a is the scattering length of the NN potential. Then the cross section can be simply expressed as

$$\sigma_{\text{tot}} = \frac{g_A^2}{\sqrt{2}\pi f_\pi^2 m_\pi^2}|J|^2 I(E_f), \tag{57}$$

where

$$|J|^2 = |J_{-1}^{\text{Born}}+J_{+1}^{\text{res}}|^2, \tag{58a}$$

$$I(E_f) = \int_0^{E_f} dE_{p'}\frac{\sqrt{E_f-E_{p'}}\sqrt{E_{p'}}}{1+m_N a^2 E_{p'}}. \tag{58b}$$

Under the approximation (56), the energy dependence of the cross section is solely given by $I(E_f)$, which incorporates the phase space and the final state interaction effect (in the Watson approximation [31]).

We have calculated the integrals J_{-1}^{Born} and J_{+1}^{res} for representative nuclear potentials: the Hamada-Johnston (HJ) potential [32], and the Reid soft-core potential (RSC) [33]. The results are given in Table I, and the corresponding cross sections are presented in Table II. These results indicate that, for the nuclear potentials considered here, the value of $|J|$ is much too small to reproduce the experimental cross section. If we define the discrepancy ratio R by

$$R \equiv \sigma_{\text{tot}}^{\text{exp}}/\sigma_{\text{tot}}^{\text{calc}}, \tag{59}$$

with $\sigma_{\text{tot}}^{\text{exp}}$ taken from Ref. [1], then $R\cong 80$ ($R\cong 210$) for the Hamada-Johnston (Reid soft-core) potential, and R happens to be almost constant for the whole range of $E_f \leqslant 23$ MeV for which $\sigma_{\text{tot}}^{\text{exp}}$ is known. Thus, although the off-shell behavior of the s-wave pion scattering amplitude derived from the chiral Lagrangian does enhance the contribution of the rescattering process over the value reported in the literature, the sign change that occurs in κ as one goes from κ_0 [Eq. (22)] to κ_{th} [Eq. (32)] results in a significant cancellation between the Born term J_{-1}^{Born} and the rescattering term J_{+1}^{res}, leading to the very small cross sections in Table II [34]. The drastic cancellation between J_{-1}^{Born} and J_{+1}^{res} found here means that the calculated cross sections are highly sensitive to the various approximations used in our calculation and also to the precise values of the constants c_1, c_2, and c_3 of Eq. (21). We will discuss these two questions in the next two paragraphs.

We adopted the threshold kinematics approximation and neglected the energy-momentum dependence in Eq. (20) and treated the vertices in Figs. 1 and 2 as fixed numbers, i.e., $\kappa(k,q) = \kappa_{\text{th}} =$ constant. In addition, although the loop corrections of chiral order $\nu = 1$, shown in Fig. 3(a), automatically introduces energy-momentum dependent vertices,

TABLE II. The total cross sections (in μb) as functions of $\eta \equiv \sqrt{2E_f/m_\pi}$, calculated with the Hamada-Johnston (HJ) and Reid soft-core (RSC) potentials.

η	$\sigma_{\rm HJ}$	$\sigma_{\rm RSC}$
0.03	0.0000	0.0000
0.06	0.0003	0.0001
0.09	0.0011	0.0004
0.12	0.0024	0.0009
0.15	0.0043	0.0016
0.18	0.0069	0.0026
0.21	0.0100	0.0037
0.24	0.0138	0.0052
0.27	0.0182	0.0068
0.30	0.0232	0.0087
0.33	0.0289	0.0108
0.36	0.0352	0.0131
0.39	0.0421	0.0157
0.42	0.0496	0.0185
0.45	0.0577	0.0215
0.48	0.0665	0.0248
0.51	0.0759	0.0283
0.54	0.0859	0.0320
0.57	0.0965	0.0360
0.60	0.1078	0.0402

we ignored this feature. The fact that the kinematics of the reaction Eq. (1) requires highly off-shell vertices leads to the expectation that the vertex form factors can be very important and invalidate the *threshold kinematics approximation* leading to Eq. (51). In this connection we note that a momentum-space calculation [13], which is free from this approximation, indicates that even a negative value of λ_1 could lead to the moderate enhancement of the cross section.

The strong cancellation between the Born and rescattering terms also means that, even within the framework of the *fixed kinematics approximation*, the large errors that exist in the empirical value of a^+ and the c_1, c_2, and c_3 constants can influence the cross sections significantly. To assess this influence, we rewrite Eq. (32) as

$$\kappa_{\rm th}=\frac{m_\pi^2}{f_\pi^2}c_1-\pi\left(1+\frac{m_\pi}{m_N}\right)a^+ +\frac{3g_A^2 m_\pi^3}{256\pi f_\pi^4}. \tag{60}$$

The use of the experimental values for a^+ and c_1 quoted earlier leads to

$$\kappa_{\rm th}=(-1.5\pm 0.4)\ \ {\rm GeV}^{-1}. \tag{61}$$

With this uncertainty taken into account, the ratio R ranges from $R=25$ to $R=2100$ for the Hamada-Johnston potential, and from $R=50$ to $R=3.4\times 10^4$ for the Reid soft-core potential. To further examine the uncertainties in the $\mathscr{L}^{(1)}$ constants we remark that the value of c_2+c_3 can be extracted from the known pion-nucleon effective range parameter b^+. The low energy pion-nucleon scattering amplitude is expanded as

$$f^+=a^+ +b^+\mathbf{q}^2+\cdots, \tag{62}$$

where $\mathbf{q}$ is the pion momentum and $b^+=(-0.044\pm 0.007)m_\pi^{-3}$ [7]. If we use $\mathscr{L}^{(1)}$ to calculate the s-wave pion-nucleon amplitude we find

$$b^+=\frac{1}{2\pi}\left(1+\frac{m_\pi}{m_N}\right)^{-1}\left(\frac{m_\pi}{f_\pi}\right)^2\left(c_2+c_3-\frac{g_A^2}{8m_N}\right)\frac{1}{m_\pi^2}, \tag{63}$$

and then Eq. (32) leads to

$$\kappa_{\rm th}=\frac{2m_\pi^2}{f_\pi^2}c_1-\pi m_\pi^2\left(1+\frac{m_\pi}{m_N}\right)b^+=(-2.7\pm 0.6)\ {\rm GeV}^{-1}. \tag{64}$$

Since c_3 is given directly by the experimental quantity α_A [Eq. (21d)], we consider Eq. (63) as an alternative input to determine c_2 in terms of b^+ and c_3. Then Eqs. (63), (21d), and the experimental value of b^+ [7] give

$$c_2=(4.5\pm 0.7)\quad {\rm GeV}^{-1}. \tag{65}$$

We note that this value is larger than the one given in Eq. (21g), indicating that the determination of c_2 requires further studies. With the new value of $\kappa_{\rm th}$ given in Eq. (64) we find that the discrepancy ratio R [Eq. (59)] can be as small as ~ 10. (In this case $|J^{\rm res}_{+1}|>|J^{\rm Born}_{-1}|$; the exact cancellation between the Born and the pion rescattering term occurs for $\kappa_{\rm th}\sim -2\ {\rm GeV}^{-1}$.)

Without attaching any significance to the detailed numbers above, we still learn the extreme sensitivity of $\sigma_{\rm tot}^{\rm calc}$ to the input parameters and that, despite this high sensitivity, $\sigma_{\rm tot}^{\rm calc}$ still falls far short of $\sigma_{\rm tot}^{\rm exp}$ (within the framework of the *fixed kinematics approximation*).

VII. DISCUSSION AND CONCLUSIONS

In this work we have used χPT to calculate the effective pion-exchange current contribution to the $pp\to pp\pi^0$ reaction at threshold. As stated repeatedly, our aim here is to carry out a systematic treatment of $\mathscr{T}$ up to chiral order $\nu=1$ [see Eq. (36)]. However, in order to make contact with the expressions appearing in the literature [3], let us consider a very limited number of $\nu=2$ diagrams. To be specific, we consider a diagram in Fig. 2(b) but with the $\overline{\nu}=0$ (p-wave) πNN vertex replaced with a $\overline{\nu}=1$ (s-wave) vertex. Then, instead of Eq. (51b), we will obtain

$$\mathscr{T}^{\rm res}_{1+2}=-\frac{g_A}{f_\pi}\kappa_{\rm th}\boldsymbol{\Sigma}\cdot\left[\hat{\mathbf{r}}f'(r)\left(2+\frac{m_\pi}{2m_N}\right)+f(r)\frac{m_\pi}{m_N}\nabla_r\right], \tag{66}$$

which is the two-body transition operator used in Ref. [3]. Thus we do recover the usual phenomenological parameterization in χPT, but this is just one of many $\nu=2$ diagrams. Our systematic $\nu=1$ calculation excludes all $\nu=2$ diagrams.

We have also ignored the exchange current contributions from scalar and vector two-nucleon exchanges. Following the χPT of Refs. [17,18] the vector meson exchange is largely accounted for via the four-nucleon contact terms illustrated in Fig. 4(a). If we had retained the last two terms of

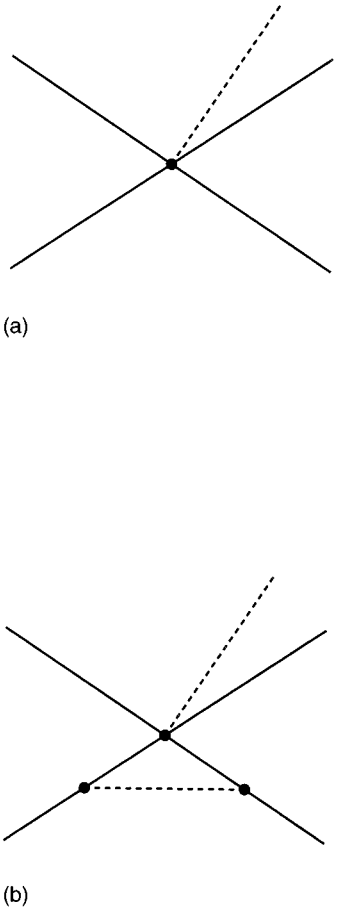

FIG. 4. Generic four-fermion-pion vertex (contact term) (a) and an example of a loop correction to a contact term (b).

Eq. (12), the pion-nucleon interaction $\mathscr{H}_{\rm int}^{(1)}$, Eq. (18b), would have had an additional piece $\mathscr{H}_{\rm int}^{(1)'}$

$$\mathscr{H}_{\rm int}^{(1)'} = \frac{c_9}{4m_N f_\pi}(\bar{N}N)[\bar{N}\boldsymbol{\sigma}\cdot\nabla(\boldsymbol{\tau}\cdot\boldsymbol{\pi})N] + \frac{c_{10}}{4m_N f_\pi}(\bar{N}\boldsymbol{\sigma}N)\cdot[\bar{N}\nabla(\boldsymbol{\tau}\cdot\boldsymbol{\pi})N]. \tag{67}$$

The $\mathscr{H}_{\rm int}^{(1)'}$ term of Fig. 4(a) has a $\boldsymbol{\sigma}\cdot\boldsymbol{q}$ structure, which means it describes p-wave pion production and therefore does not contribute to the threshold $pp \to pp\pi^0$ reaction. The s-wave pion production contact term, also belonging to the type of diagram illustrated in Fig. 4(a), enters as a $1/m_N$ recoil correction to $\mathscr{H}_{\rm int}^{(1)'}$ and therefore is of chiral order $\nu = 2$. Formally, the chiral order $\nu=2$ diagrams have no place in the present calculation limited to $\nu=1$. However, in view of the great current interest in the possible large contribution of the heavy-meson exchange diagrams, we make a few remarks on the s-wave $\nu=2$ contact terms depicted in Fig. 4(a). We note that the coordinate representation of this contact term contains $\delta^3(\boldsymbol{r})$. Meanwhile, in the threshold $pp \to pp\pi^0$ reaction the initial two-nucleon relative motion must be in p wave (because of parity) and so its wave function vanishes at $\boldsymbol{r}=0$. Thus, even in a chiral order $\nu=2$ calculation, the contact term Fig. 4(a) corresponding to s-wave pion production will play no role. Including meson loops corrections to these contact terms [an example illustrated in Fig. 4(b)] would smear out the δ-function behavior, allowing them to have a finite contribution to the threshold $pp \to pp\pi^0$ reaction. This involves, however, diagrams of even higher chiral order than $\nu=2$. Thus, in order to include the strong effective isoscalar-vector repulsion of the N-N forces (ω exchange) contained in the four-nucleon contact terms of Weinberg's [17] and van Kolck's *et al.*'s [18] χPT description, we have to go to chiral order $\nu=3$.

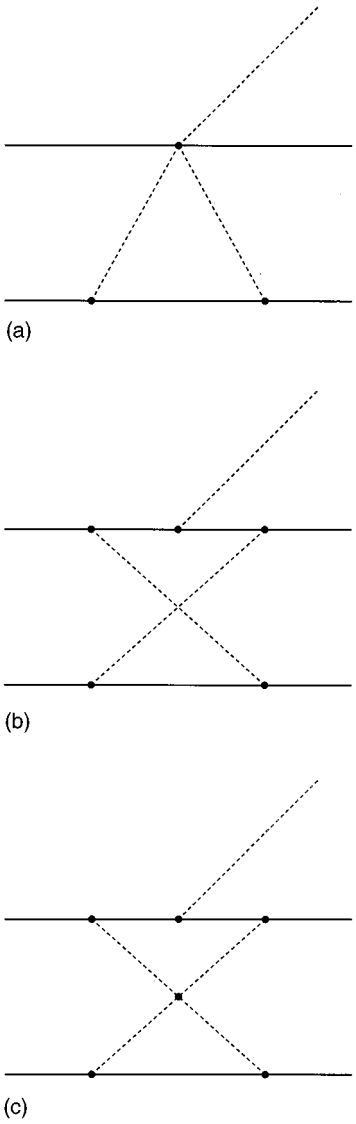

FIG. 5. A few higher order diagrams contributing to the effective two-nucleon scalar exchange in nuclear χPT.

Meanwhile, one may picture the ''effective heavy mesons'' as generated by multipion exchange diagrams like those illustrated in Fig. 5. These diagrams, which necessarily contain loops, represent a very limited class of $\nu \geqslant 3$ diagrams. For example, an important part of the effective scalar exchange between two nucleons involve intermediate π-π s-wave interaction which requires at least two loop diagrams like Fig. 5(c). Thus, if we are to interpret the heavy-meson exchange diagrams of Lee and Riska [8] in the framework of

nuclear χPT, we must deal with terms with chiral order $\nu \geqslant 3$, which at present is beyond practical calculations.

We now recapitulate the main points of this article.

(1) Using χPT in a systematic fashion we have shown that the contribution of the pion rescattering term can be much larger than obtained in the traditional phenomenological calculations. This fact itself supports the suggestion of Hernandez and Oset [11] that the off-shell *s*-wave pion-nucleon scattering should enhance the rescattering contribution significantly. However, the sign of the enhanced rescattering vertex obtained in χPT is *opposite* to that used in Ref. [11], at least for the *typical threshold kinematics* defined in the text. This sign change in the coupling constant κ_{th} leads to a destructive interference between the Born and rescattering terms instead of the constructive interference found in Ref. [11]. The significant cancellation between these terms give rise to the very small cross section for the near-threshold $pp \to pp\pi^0$ reaction calculated in this work. Although our particular numerical results were obtained in what we call the *fixed kinematics approximation*, these results at least indicate that the large enhancement of $\sigma_{\rm tot}^{\rm calc}$ obtained in Ref. [11] is open to more detailed examinations.

(2) The *fixed kinematics approximation* (which is commonly used in the literature) should be avoided. There are at least two reasons why this is not a good approximation for this reaction: (i) the initial- and final-state interactions play an essential role in the near-threshold $pp \to pp\pi^0$ reaction; (ii) the theoretical cross section within the framework of the Born plus rescattering terms is likely to depend on the delicate cancellation between these two terms. In a momentum space calculation [13], we can easily avoid the *fixed kinematics approximation*. Such a calculation will allow us to work with full off-shell kinematics, to incorporate the χPT form factors in the Born term, and to reduce ambiguities in our calculation down to the level of uncertainties in the input parameters in χPT and the chiral counter terms.

(3) Several works [8,10,13] indicate that the two-nucleon scalar (σ) exchange can be very important. We gave in the introduction a simple kinematical argument for its plausibility, and our dynamical calculation (albeit of semiquantitative nature) seems to indicate the necessity of the σ exchange contribution in order to explain the observed cross sections for the threshold $pp \to pp\pi^0$ reaction. It is of great interest to see to what extent an improved χPT calculation based on momentum-space representation helps sharpen the conclusion on the necessity of the sigma exchange diagram. Such a calculation is now in progress. If it is established that the heavy meson exchange diagrams play an essential role in the threshold $pp \to pp\pi^0$ reaction, it seems that we must resort to a modified version of χPT, for a brute force extension of our treatment to $\nu \geqslant 2$ seems extremely difficult. An attempt to include vector meson degrees of freedoms explicitly can be found, e.g., in Ref. [19]. A purely phenomenological approach as used in [8] may also be a useful alternative.

ACKNOWLEDGMENTS

We are grateful to U. van Kolck for the useful communication on Ref. [22]. One of us (B.-Y.P.) is grateful for the hospitality of the Nuclear Theory Group of the University of South Carolina, where the main part of this work was done. This work is supported in part by the National Science Foundation, Grant No. PHYS-9310124.

[1] H. O. Meyer *et al.*, Phys. Rev. Lett. **65**, 2846 (1990); Nucl. Phys. **A539**, 633 (1992).
[2] A. Bondar *et al.*, Phys. Lett. B **356**, 8 (1995).
[3] D. S. Koltun and A. Reitan, Phys. Rev. **141**, 1413 (1966).
[4] G. A. Miller and P. U. Sauer, Phys. Rev. C **44**, R1725 (1991).
[5] J. A. Niskanen, Phys. Lett. B **289**, 227 (1992).
[6] S. Weinberg, Phys. Rev. Lett. **17**, 616 (1966).
[7] G. Höhler, in *Pion-Nucleon Scattering*, edited by K. H. Hellwege, Landolt-Börnstein, New Series, Group I, Vol. 9, b2 (Springer-Verlag, New York, 1983).
[8] T.-S. H. Lee and D. O. Riska, Phys. Rev. Lett. **70**, 2237 (1993).
[9] P. G. Blunden and D. O. Riska, Nucl. Phys. **A536**, 697 (1992); K. Tsushima, D. O. Riska, and P. G. Blunden, *ibid.* **559**, 543 (1993).
[10] C. J. Horowitz, H. O. Meyer, and D. K. Griegel, Phys. Rev. C **49**, 1337 (1994).
[11] E. Hernández and E. Oset, Phys. Lett. B **350**, 158 (1995).
[12] G. Hamilton, in *High Energy Physics*, edited by E. H. S. Burhop (Academic Press, New York, 1967), Vol. 1, p. 194.
[13] C. Hanhart, J. Haidenbauer, A. Reuber, C. Schütz, and J. Speth, Phys. Lett. B **358**, 21 (1995).
[14] J. Gasser and H. Leutwyler, Ann. Phys. (N.Y.) **158**, 142 (1984).
[15] For a review, see e.g., V. Bernard, N. Kaiser, and Ulf-G. Meissner, Int. J. Mod. Phys. E **4**, 193 (1995)
[16] E. Jenkins and A. V. Manohar, Phys. Lett. B **255**, 558 (1991).
[17] S. Weinberg, Phys. Lett. B **251**, 288 (1990); Nucl. Phys. **B363**, 3 (1991); Phys. Lett. B **295**, 114 (1992).
[18] U. van Kolck, thesis, University of Texas at Austin, 1992; C. Ordonez, L. Ray, and U. van Kolck, Phys. Rev. Lett. **72**, 1982 (1994).
[19] T. S. Park, D.-P. Min, and M. Rho, Phys. Rep. **233**, 341 (1993).
[20] T. S. Park, I. S. Towner, and K. Kubodera, Nucl. Phys. **A579**, 381 (1994).
[21] T. S. Park, D.-P. Min, and M. Rho, Phys. Rev. Lett. **74**, 4153 (1995); "Chiral Lagrangian approach to exchange vector currents in nuclei," Report No. SNUTP 95-043 (nucl-th/9505017), 1995.
[22] T. D. Cohen, J. L. Friar, G. A. Miller, and U. van Kolck, "The $pp \to pp\pi^0$ Reaction Near Threshold: A Chiral Power Counting Approach," nucl-th/9512036.
[23] See, e.g., H. Georgi, *Weak Interactions and Modern Particle Theory* (Benjamin, New York, 1984).
[24] This is the form used by Bernard *et al.* [15]. Another commonly used parameterization is the "exponential form," see, e.g. [19,23], where $U(x) = \exp[i\boldsymbol{\tau}\cdot\boldsymbol{\pi}(x)/f_\pi]$.
[25] In practical calculations we will choose the nucleon rest frame $v_\mu = (1,\mathbf{0})$ in which case Eq. (7) corresponds to the standard nonrelativistic reduction of a spinor into upper and lower components and the covariant spin operator of Eq. (16) is simply given by $S = (0, \frac{1}{2}\boldsymbol{\sigma})$.

[26] In Eq. (11a) the sum over A runs over the possible combinations of γ and $\boldsymbol{\tau}$ matrices: $\Gamma_S^S=1$, $\Gamma_S^V=\boldsymbol{\tau}$, $\Gamma_V^S=S_\mu$, and $\Gamma_V^V=S_\mu\boldsymbol{\tau}$. However, because of the Fermi statistics (Fierz rearrangement), only two of the four coupling constants C_A are independent.

[27] V. Bernard, N. Kaiser, and Ulf-G. Meissner, Phys. Lett. B **309**, 421 (1993).

[28] J. Gasser, H. Leutwyler, and M. E. Sainio, Phys. Lett. B **253**, 252, 260 (1991).

[29] R. Koch, Nucl. Phys. **A448**, 707 (1986).

[30] We may remark in passing that this ''standard value'' for λ_1 determined from a^+, is numerically close to the contribution of the crossed Born term, which in HFF is grouped with the c_2 term in $\mathscr{L}^{(1)}$ as $g_A^2/8m_N$. This remnant of the s-wave pion nucleon crossed Born term in HFF, appears in the second term in Eq. (23), and gives a value of a^+,

$$a^+=-\frac{1}{2\pi}\left(1+\frac{m_\pi}{m_N}\right)\frac{m_\pi^2}{f_\pi^2}\frac{g_A^2}{8m_N}\approx-0.009m_\pi^{-1}$$

compatible with $a^+_{\rm exp}=(-0.83\pm0.38)\times10^{-2}m_\pi^{-1}$ [7].

[31] K. M. Watson, Phys. Rev. **88**, 1163 (1952).

[32] T. Hamada and I. D. Johnston, Nucl. Phys. **34**, 382 (1962).

[33] R. V. Reid, Ann. Phys. **50**, 411 (1968).

[34] This type of cancellation has also been noted in [22].